CUED - Engineering Tripos Part IIB 2024-2025 **Module Coursework**

Module	4G10	Title of report	4G10 Coursework 1
Date submitted: 21 Nov		Assessment for this module is ☑ 100% / ☐ 25% coursework of which this assignment forms 50 %	

UNDERGRADUATE and POST GRADUATE STUDENTS		
Candidate number:	5641G	☑ Undergraduate ☐ Post graduate

Feedback to the student ☐ **See also comments in the text**		Very good	**Good**	Needs improvmt
CONTENT	**Completeness, quantity of content:** Has the report covered all aspects of the lab? Has the analysis been carried out thoroughly?			
	Correctness, quality of content Is the data correct? Is the analysis of the data correct? Are the conclusions correct?			
	Depth of understanding, quality of discussion Does the report show a good technical understanding? Have all the relevant conclusions been drawn?			
	Comments:			
PRESENTATION	**Attention to detail, typesetting and typographical errors** Is the report free of typographical errors? Are the figures/tables/references presented professionally?			
	Comments:			

Marker: Date:

1 Plotting raw PSTHs

Panel a,b,c in Figure 1 show the PSTH of all neurons under several specific conditions. All neurons remained stable at a low firing rate below 20 Hz before −200 ms. Around −200 ms, the firing rate of some neurons rapidly increased, corresponding to the 'go cue' and the monkey's preparation for movement.

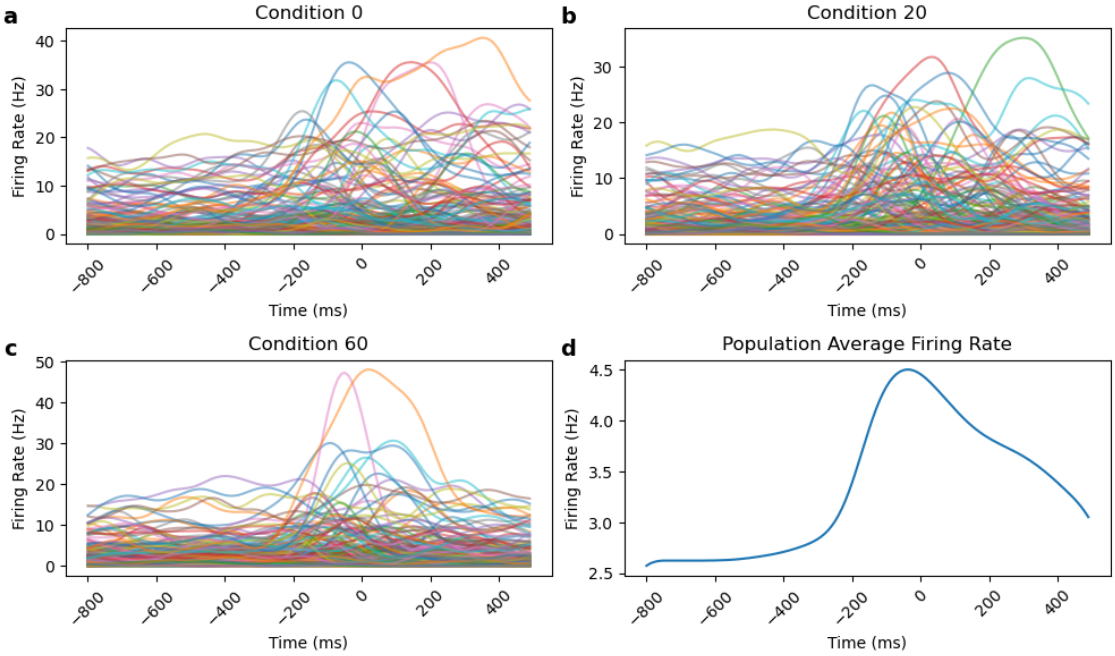

Figure 1: **Panel a,b,c:** PSTH plots showing firing rate of all neurons under certain conditions. **Panel d:** Population firing rate (averaged across neurons and conditions).

The population firing rate, as shown in Panel d of Figure 1, starts to rise significantly above its baseline level (2.6 Hz) approximately 250 ms before movement onset. Possible explanation is reaction time. There is likely a delay between the go-cue signal and the actual movement onset, corresponding to the monkey's reaction time, during which neural activity begins to ramp up in preparation for motor execution.

2 Preprocessing

(a) Normalization of PSTH

The PSTH for each neuron is normalized using the following formula:

$$\text{psth} = \frac{\text{psth} - b}{a - b + 5}$$

where a and b are the maximum and minimum firing rates of the neuron across all times and conditions. The resulting normalized values are plotted in Figure 2 (left panel). Normalization could have several purposes:

1. **Removal of Baseline Variation:** Neurons exhibit diverse baseline firing rates, ranging from 5 to 20 spikes per second. The subtraction of b (psth $- b$) removes this baseline variation, ensuring that differences in neural activity are not dominated by baseline offsets (see Figure 2 panels a, b, and c).

2. **Consistent Activity Range:** Dividing by the range $(a - b + 5)$ ensures that the normalized PSTH values have a consistent scale across neurons. This is important because neurons have varying activity amplitudes, as shown in left panel of Figure 2, the majority of neurons have a maximum firing rate below 20, while a few neurons reach values as high as 40 or even 70.

3. **Facilitating Principal Component Analysis:** The computation of covariance matrix in PCA is sensitive to the scale of the data. Without normalization, neurons with higher firing rates would dominate the analysis.

The normalised PSTH array is then centered by removing its cross-condition mean.

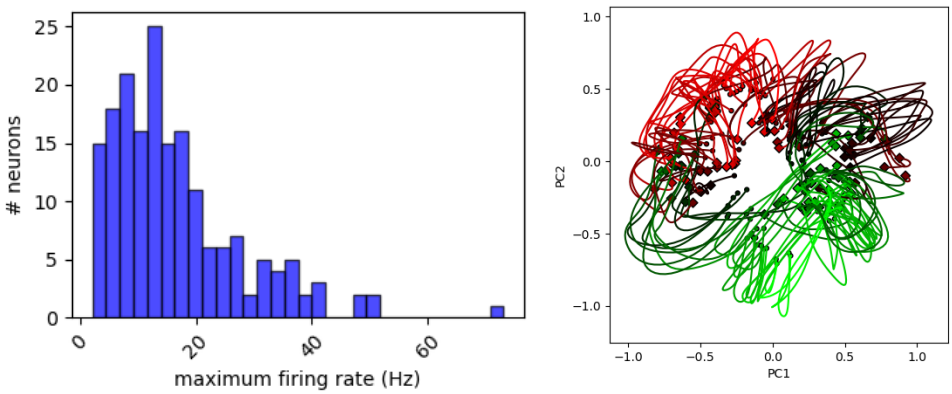

Figure 2: **Left:** Histogram of the neurons' maximum firing rate. **Right:** Trajectories of neural activity in the PC1-PC2 plane.

(c) Dimensionality Reduction using PCA

The normalized, mean-centered, and time-trimmed PSTH data $\mathbf{X}$ is in shape of $N \times CT$, where N is the number of neurons, C is the number of conditions, and $T = 46$ is the number of time bins. The goal of PCA is to project the high-dimensional data (dim=N=182) into a lower-dimensional space (dim=M=12) that captures the most significant variance in the data.

Approximate the covariance matrix of $\mathbf{X}$ from data and apply eigenvalue decomposition:

$$\text{Cov}(\mathbf{X}) \approx \frac{1}{CT}\mathbf{X}\mathbf{X}^\top = \mathbf{V}_M \Lambda \mathbf{V}_M^\top$$

where Λ is an $M \times M$ diagonal matrix containing the M largest eigenvalues λ_i, and $\mathbf{V}_M$ is an $N \times M$ matrix whose columns are the corresponding eigenvectors. To obtain the low-dimensional representation $\mathbf{Z}$ (of shape $M \times CT$), $\mathbf{X}$ is projected onto the first M principal components:

$$\mathbf{Z} = \mathbf{V}_M^\top \mathbf{X},$$

3 Plotting PC Space Trajectories

The trajectories of neural activity in the PC1-PC2 plane were plotted in the right panel of Figure 2. Each trajectory corresponds to a condition, with colors assigned based on the initial points of the trajectories at -150 ms using the cond_color.get_colors function.

4 Maximum-likelihood Estimation for A

(a) Log-likelihood of A and its naive gradient

The latent rotation trajectory is modeled as below. $\mathbf{z_t^{(c)}}$ denote an $M \times 1$ vector at a given time t and under a certain condition c. For simplicity, notation c is ignored.

$$\Delta \mathbf{z}_{t+1} = \mathbf{A}\mathbf{z}_t + \sigma\epsilon_t \quad \text{with } \epsilon_t \sim \mathcal{N}(\mathbf{0}, \mathbf{I})$$

$$\mathbf{z}_{t+1} = \mathbf{z}_t + \Delta \mathbf{z}_{t+1}$$

$\Delta\mathbf{z}$ is given by taking differences of $\mathbf{z}$ across time. In practical calculations, $\Delta\mathbf{Z}$ therefore would have only $(T-1) = 45$ time points, where the first time point is $\Delta\mathbf{z}_2 = \Delta\mathbf{z}_2 - \Delta\mathbf{z}_1 = \mathbf{A}\mathbf{z}_1 + \sigma\epsilon_1$. To ensure same matrix shape, in the practical calculation, the first $(T-1)$ time points of $\mathbf{Z}$ are taken. Now both $\mathbf{Z}$ and $\Delta\mathbf{Z}$ is of shape $M \times CT$.

The log-likelihood of getting $\mathbf{Z}$ given $\mathbf{A}$ is:

$$\log \mathcal{L}(\theta, \mathbf{Z}) = \log P(\mathbf{Z}|\mathbf{A}) = \log P(\Delta\mathbf{Z} - \mathbf{A}\mathbf{Z}|\mathbf{A}) \tag{1}$$

$$= \sum_c \sum_{t=1}^{T-1} \log \mathcal{N}(\Delta\mathbf{z}_{t+1} - \mathbf{A}\mathbf{z}_t; \mathbf{0}, \sigma^2\mathbf{I}) \tag{2}$$

$$= \sum_c \sum_{t=1}^{T-1} \left[-\frac{M}{2}\log(2\pi) - \frac{M}{2}\log(\sigma^2) - \frac{1}{2\sigma^2}(\Delta\mathbf{z}_{t+1} - \mathbf{A}\mathbf{z}_t)^\top(\Delta\mathbf{z}_{t+1} - \mathbf{A}\mathbf{z}_t) \right]. \tag{3}$$

Ignoring terms independent of $\mathbf{A}$ and setting $\sigma = 1$, the simplified log-likelihood becomes:

$$\log \mathcal{L}(\theta, \mathbf{Z}) = -\frac{1}{2}\sum_c \sum_{t=1}^{T-1} (\Delta\mathbf{z}_{t+1} - \mathbf{A}\mathbf{z}_t)^\top(\Delta\mathbf{z}_{t+1} - \mathbf{A}\mathbf{z}_t) + \text{const.}$$

To compute the gradient, we write the log-likelihood in index notation:

$$\frac{\partial \log \mathcal{L}(\theta, \mathbf{Z})}{\partial A_{ij}} = -\frac{1}{2}\sum_c \sum_{t=1}^{T-1} \frac{\partial}{\partial A_{ij}} \Big[-\Delta z_{t+1,k} A_{kl} z_{t,l} - z_{t,k} A_{lk} \Delta z_{t+1,l} + z_{t,k} A_{lk} A_{lm} z_{t,m} \Big] \tag{4}$$

$$= \sum_c \sum_{t=1}^{T-1} \Big[\Delta z_{t+1,i} z_{t,j} - z_{t,j} A_{im} z_{t,m} \Big]. \tag{5}$$

Returning to matrix form, the gradient of the log-likelihood becomes:

$$\frac{\partial \log \mathcal{L}(\theta, \mathbf{Z})}{\partial \mathbf{A}} = \sum_c \sum_{t=1}^{T-1} \left[\Delta\mathbf{z}_{t+1}\mathbf{z}_t^\top - \mathbf{A}\mathbf{z}_t\mathbf{z}_t^\top \right] \tag{6}$$

$$= \Delta\mathbf{Z}\mathbf{Z}^\top - \mathbf{A}\mathbf{Z}\mathbf{Z}^\top. \tag{7}$$

This result provides the gradient of the log-likelihood with respect to $\mathbf{A}$, which can be used for optimization.

(b) Parametrising an Antisymmetric A

Since $\mathbf{A}$ must be antisymmetric, the number of independent parameters is reduced from M^2 to $K = \frac{M^2 - M}{2}$, where K represents the number of unique above-diagonal entries in $\mathbf{A}$. For $M = 12$, this gives $K = 66$.

To ensure antisymmetry, $\mathbf{A}$ is constructed using a K-dim vector β and a coefficient tensor H_{aij} as follows:

$$A_{ij} = \sum_{a=1}^{K} \beta_a H_{aij} \text{ , where } H_{aij} = \begin{cases} 1 & \text{if } j > i, \\ -1 & \text{if } j < i, \\ 0 & \text{otherwise.} \end{cases}$$

By setting $M = 4$ and $K = 6$, with $\beta = [1, 2, 3, 4, 5, 6]$, the constructed $\mathbf{A}$ is:

$$\mathbf{A} = \begin{bmatrix} 0 & 1 & 2 & 3 \\ -1 & 0 & 4 & 5 \\ -2 & -4 & 0 & 6 \\ -3 & -5 & -6 & 0 \end{bmatrix}.$$

This result confirms that $\mathbf{A}$ is antisymmetric, as required. By expressing $\mathbf{A}$ in terms of β and H, the antisymmetric constraint is naturally enforced, simplifying the optimization process.

(c) Gradient with respect to β

The gradient of the log-likelihood with respect to β is derived by substituting the antisymmetric parameterisation of $\mathbf{A}$ into the expression for the gradient. Using the previously obtained result for $\frac{\partial \log \mathcal{L}(\theta, \mathbf{Z})}{\partial \mathbf{A}}$, we express $A_{im} = \beta_b H_{bim}$ and define $\mathbf{W}_t = \mathbf{H}\mathbf{z}_t$, where $\mathbf{W}_t$ is a (K, M) matrix for a given condition c and time t. Starting from index notation:

$$\frac{\partial \log \mathcal{L}(\theta, \mathbf{Z})}{\partial \beta_a} = \frac{\partial \log \mathcal{L}(\theta, \mathbf{Z})}{\partial A_{ij}} \frac{\partial A_{ij}}{\partial \beta_a} = \frac{\partial \log \mathcal{L}(\theta, \mathbf{Z})}{\partial A_{ij}} H_{aij} \tag{8}$$

$$= \sum_c \sum_{t=1}^{(T-1)} \left[\Delta z_{t+1,i} H_{aij} z_{t,j} - H_{aij} z_{t,j} \beta_b H_{bim} z_{t,m} \right] \tag{9}$$

$$= \sum_c \sum_{t=1}^{(T-1)} \left[\Delta z_{t+1,i} W_{t,ai} - W_{t,ai} \beta_b W_{t,bi} \right] \tag{10}$$

Returning to matrix form:

$$\frac{\partial \log \mathcal{L}(\theta, \mathbf{Z})}{\partial \beta} = \sum_c \sum_{t=1}^{T-1} \left[\mathbf{W}_t \Delta \mathbf{z}_{t+1} - \mathbf{W}_t \mathbf{W}_t^\top \beta \right] \tag{11}$$

$$= \mathbf{W} \Delta \mathbf{Z} - \mathbf{W}\mathbf{W}^\top \beta \tag{12}$$

$$= \mathbf{b} - \mathbf{Q}\beta \tag{13}$$

where $\mathbf{W} = \mathbf{HZ}$ is reshaped to have dimensions $(K, MC(T-1))$, and $\Delta\mathbf{Z}$ is reshaped to a column vector $(MC(T-1), 1)$. Extra notes on matrices shapes can be found in Appendix A. $\mathbf{b}$ and $\mathbf{Q}$ is defined as:

$$\mathbf{b} = \mathbf{W}\Delta\mathbf{Z}, \quad \mathbf{Q} = \mathbf{W}\mathbf{W}^\top$$

(d) An antisymmetric estimate for A

Setting the gradient to zero gives the maximum-likelihood estimation of $\mathbf{A}$. The estimated $\hat{\mathbf{A}}$ is plotted as heatmap in Figure 3.

$$\hat{\beta} = \mathbf{Q^{-1}b} = (\mathbf{W}\mathbf{W}^\top)^{-1}\mathbf{W}\boldsymbol{\Delta}\mathbf{Z}$$

$$\hat{A}_{ij} = \sum_{a=1}^{K} \hat{\beta}_a H_{aij}$$

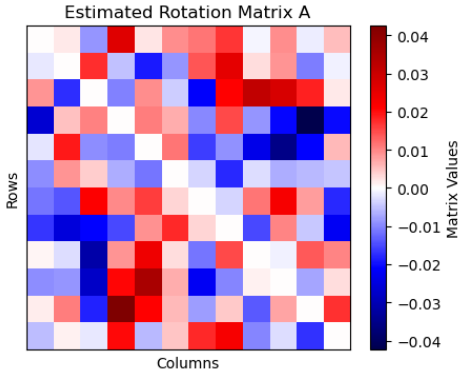

Figure 3: Visualisation of $\hat{\mathbf{A}}$ estimated from psths.npz.

(e) Test

The matrix $\hat{\mathbf{A}}_{\text{test}}$ was estimated from the test data $\mathbf{Z}_{\text{test}}$ using the derived methods. The maximum absolute difference between the elements of $\hat{\mathbf{A}}_{\text{test}}$ and groundtruth $\mathbf{A}_{\text{test}}$ was computed to be less than 2.7×10^{-12}.

5 2D projections with rotational dynamics

(a) Angular Speeds and Eigenvectors

The eigenvalues of the antisymmetric matrix $\mathbf{A}$ were computed, and their imaginary parts were used to determine the angular speeds ω for the rotations in six orthogonal 2D planes. The resulting angular speeds are shown below.

$$\omega = [0.092, 0.067, 0.045, 0.016, 0.011, 0.003] \text{ rad/10ms}$$

(b) 2D Projection onto the Fastest Rotation (FR) Plane

The first angular speed ($\omega = 0.092$ rad/10ms) is the largest and corresponds to the fastest rotation plane, which is spanned by the eigenvector associated with the first pair of eigenvalues. The complex eigenvector $\mathbf{v}$ is normalized such that $\|\mathbf{v}\| = 1$. To extract the real and imaginary components for constructing the 2D plane, each part is further normalized individually:

$$\mathbf{u}_R = \frac{\text{Re}(\mathbf{v})}{\|\text{Re}(\mathbf{v})\|}, \quad \mathbf{u}_I = \frac{\text{Im}(\mathbf{v})}{\|\text{Im}(\mathbf{v})\|}.$$

The 2D projection of the latent trajectory $\mathbf{Z}$ onto the plane of the fastest rotation (FR plane) is given by:

$$\mathbf{P}_{FR}\mathbf{Z} = \begin{bmatrix}\mathbf{u}_R & \mathbf{u}_I\end{bmatrix}^\top \mathbf{Z},$$

where $\mathbf{P}_{FR}$ is the projection matrix constructed from the normalized real and imaginary parts of the eigenvector. This projection maps the M-dimensional latent trajectory $\mathbf{Z}$ into a 2D subspace representing the FR plane.

(c) 2D Projections onto the first FR plane

The trajectories of the latent variables $\mathbf{Z}$ were projected onto the first FR plane corresponding to the largest angular speed $\omega = 0.092$ rad/10ms. Left panel of Figure 4 shows the resulting projections. The projection reveals a prominent rotational pattern. Within [−150ms,+200ms], the trajectory completes slightly more than a half-circle, consistent with the angular speed. The expected rotation angle can be calculated as:

$$0.092\,\text{rad/10ms} \times 35\,\text{steps} \times \frac{180}{\pi} \approx 184^\circ.$$

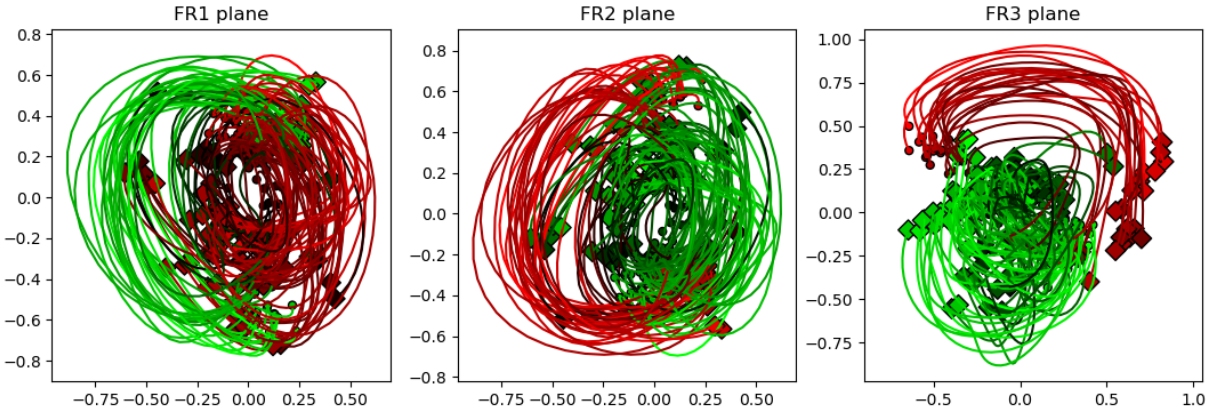

Figure 4: Projection of Z on FR planes. Angular speeds are $[0.092, 0.067, 0.045]$ rad/10ms

(d) 2D Projections onto more FR planes.

The middle and the right panel of Figure 4 present projections onto the second and the third FR planes. In comparison to the first FR plane, the projections exhibit slower angular progression over the same interval. This is expected, as the smaller angular speeds correspond to slower rotations in the associated planes.

6 Pre-Movement Period

To analyze the pre-movement period, the same projection matrix $\mathbf{P}_{FR}$ used for the movement interval was applied to the data from $[-800\,\text{ms}, -150\,\text{ms}]$. This allowed us to visualize the neural trajectories during the pre-movement period in the FR plane, as plotted in Figure 5.

Before the target onset, the monkey is unaware of the target's location. Consequently, the neural encoding remains centralized near the origin of the FR plane, and no significant differences are observed between conditions. This reflects a lack of condition-specific motor preparation during this period.

After the target onset, the monkey gains knowledge of the target's location. The projections in the FR plane shift from the origin toward the starting points of the rotational trajectories, which represent the autonomous system's initialization state. This transition indicates that the monkey begins planning its movement trace. The traces diverge between conditions, reflecting condition-specific motor plans, including how to navigate obstacles.

This pre-movement activity highlights the neural dynamics associated with motor planning. It suggests that the monkey has fully prepared its motor commands by the time movement begins, as evidenced by the divergence of traces across conditions.

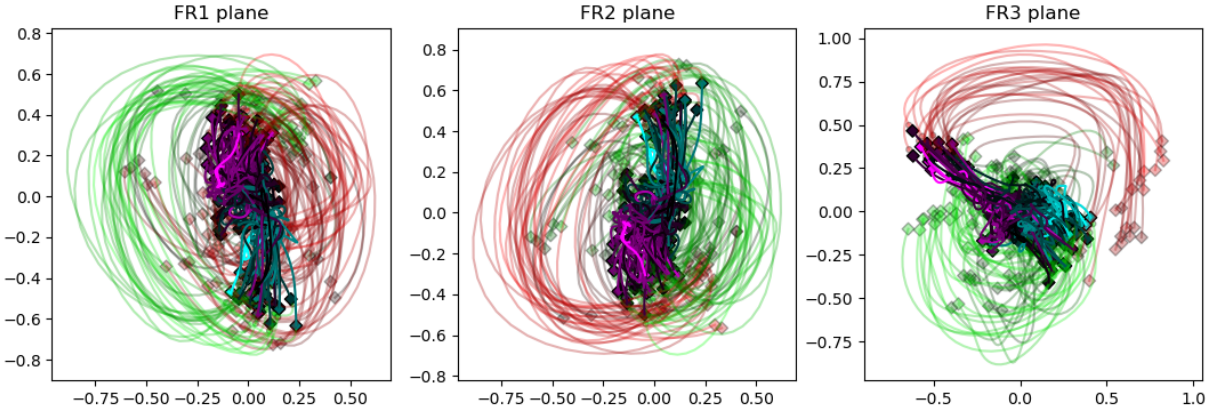

Figure 5: Projection of **Z** onto the FR planes, highlighting the pre-movement period.

7 Control Analysis

To evaluate the robustness of the rotational patterns observed in the neural trajectories, distortions were applied to the original **X**. Three different distortions were considered with the projections onto the first FR plane plotted for all in Figure 6.

1. **Distorted Data** (Left panel): The data were distorted by inverting the movement-period of the PSTHs for half of the conditions. The inverted conditions were randomly selected for each neuron. This disrupted statistical correlations between conditions and neurons, breaking rotational patterns. However, time correlations were preserved, resulting in smooth trajectories.

2. **Less Extreme Distortion** (Mid panel): PSTHs were inverted for half of the conditions, but the same conditions were inverted across all neurons. This disrupted condition correlations while preserving most neuron correlations. The resulting S-shaped trajectories retained rotational features, reflecting reversed rotation directions for inverted conditions.

3. **Extreme Distortion** (Right panel): PSTHs were inverted for half of the conditions (randomly per neuron) and shuffled along the time axis. This destroyed neuron correlations and temporal continuity, eliminating both smoothness and rotational patterns in the trajectories.

In conclusion, Figure 6 confirms the analysis. Distorted data (left panel) preserved temporal continuity but lost rotation. Less extreme distortion (mid panel) retained rotational patterns, forming S-shaped trajectories. Extreme distortion (right panel) removed both rotation and continuity. These results validate that the rotational relationships in Section 5 are genuine and rooted in neural activity, not overfitting.

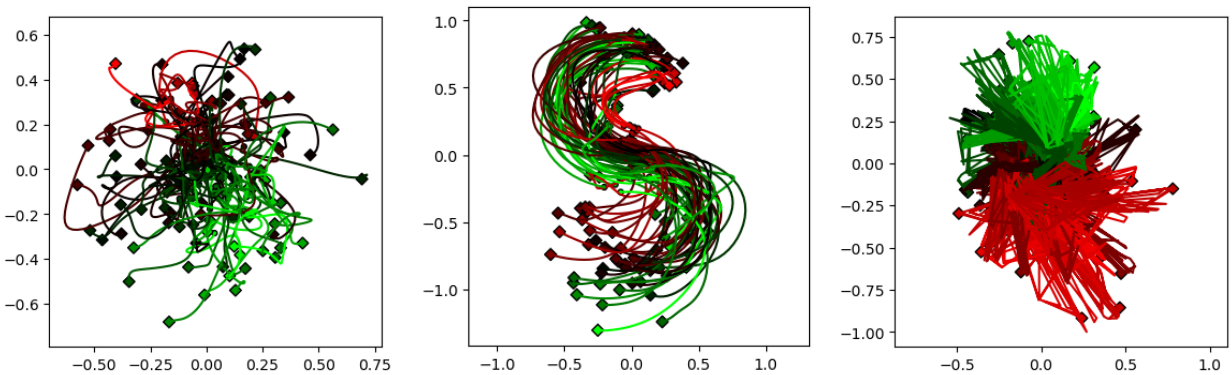

Figure 6: Projections of distorted **Z** onto the first FR plane under three conditions. **Left:** Distorted data. **Mid:** Less extreme distortion. **Right:** Extreme distortion.

Appendix

A Extra notes on matrix shapes

- **Ignoring summation over c and t.**

  $\mathbf{W}_t = \mathbf{H}\mathbf{z}_t$ has shape $(K, M) = (K, M, M) \times M$. The gradient for time t and condition c $\mathbf{W}_t \Delta \mathbf{z}_{t+1} - \mathbf{W}_t \mathbf{W}_t^\top \beta$ has shape:

  $$(K, M) \times M - (K, M) \times (M, K) \times K = (K, 1)$$

- **Considering all time points and conditions.**

  $\mathbf{W} = \mathbf{H}\mathbf{Z}$ has shape $(K, M, C(T-1)) = (K, M, M) \times (M, C(T-1))$.

  After reshaping $\mathbf{W}$ to $(K, MC(T-1))$ and reshaping $\Delta\mathbf{Z}$ to $(MC(T-1), 1)$, the final gradient $\mathbf{W}\Delta\mathbf{Z} - \mathbf{W}\mathbf{W}^\top \beta$ has shape:

  $$(K, MC(T-1)) \times (MC(T-1), 1) - (K, MC(T-1)) \times (MC(T-1), K) \times (K, 1) = (K, 1)$$

B Code

All code can be found in github repo: https://github.com/derek1909/4G10-Coursework-1.git